Coexistence of Dual Inductive Wireless Power Transfer Systems

ENEAS HÅLLSTEN
MASTER´S THESIS
DEPARTMENT OF ELECTRICAL AND INFORMATION TECHNOLOGY
FACULTY OF ENGINEERING | LTH | LUND UNIVERSITY

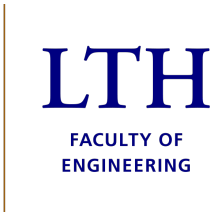

Coexistence of Dual Inductive Wireless Power Transfer Systems

Eneas Hållsten
en2225ha-s@student.lu.se

Department of Electrical and Information Technology
Lund University
In collaboration with nok9

Academic Supervisor: Professor Buon Kiong Lau

Industrial Supervisors: Laurens Swaans,
Max Andersson

Examiner: Professor Mats Gustafsson

September 7, 2022

Printed in Sweden
Tryckeriet i E-huset, Lund

Abstract

Wireless power transfer is emerging into everyday life. The idea is to create a more convenient way of charging, or at least powering, devices. Ideally, all power transmitters and power-receiving devices should be interoperable so that the user does not need to investigate whether a specific power transmitter will work together with a specific device. Interoperability is what the standard Qi, invented by the Wireless Power Consortium, has achieved for the wireless charging of smartphones since its release in 2008, which also leads to its phenomenal success. However, when it comes to cordless kitchen appliances, the standard (called Ki) is still under development; the idea is to transform the kitchen into a cordless environment, for the user's convenience. Unlike Qi, which standardizes power transfer in the order of tens of watts, Ki should safely handle power level of up to the kilowatt range. Hence, Ki is technically more challenging to develop.

This thesis investigates how the dual wireless power systems proposed in Ki may coexist in space and time. One system is used to transfer high power levels in the kilowatt range for appliance operation, while the other utilizes low power of less than 1 watt for communication needs. To simply implementation, the current Ki approach is to separate the operation of two systems in time, to bypass the need for coexistence. In this investigation, the dual wireless power systems were first characterized. It was found that the transmitting and receiving units will act significantly differently depending on the material that surrounds the power transmitter and receiving units. With the system characterized, methods to decouple the two systems (i.e., a filter and a shielding barrier) were studied. The decoupling of the two systems is important as the signals from one system can otherwise interfere with the correct operation of the other system, and vice-versa. Although coexistence has not been achieved in this work, the progress made towards that direction is presented. Adequate shielding of the combined of a low-frequency magnetic field and a high-frequency electric field will require further efforts. In addition, the low-power communication system is very susceptible to interference due to its lower signal power compared to the noise emitted by the high-power system. Increasing the power level in the low-power system may enable coexistence.

Popular Science Summary

Wireless power transfer (WPT) is an emerging field with numerous exciting research opportunities.

Today, the most common standardized WPT application is the wireless charging of small mobile devices, where the amount of power transferred is relatively small. When higher power levels are involved, such as the powering of kitchen appliances through WPT, the engineer must consider other technical aspects. For example, a high-power device that is not to be charged, but directly powered by WPT, may contain electronics within the device. Those electronics may need another power source available before or independent of the high power source.

The Wireless Power Consortium, which came up with the Qi specification for wireless charging of smartphones, has been developing a specification for kitchen appliances, called Ki. As in the case of the Qi specification, this interface utilizes inductive coupling for both power transfer and communication. However, whereas the communication in Qi is realized by modulation of the power transfer signals (so called "in-band-communication"), the communication in Ki is performed based on the NFC standard. This means that in Ki, the WPT and communication is separated both physically and electrically; two separate coils are used and will operate at different frequencies.

The receiver needs to communicate with the transmitter actively, even when the appliances are not operating with high power. Power-up or standby mode are two examples of such cases. Using the high-power coils to provide standby power is highly inefficient and adding a battery to the appliance is not the desired option. Thus, the NFC link will be utilized as a secondary low-power transfer link. One way of achieving coexistence is through time division duplex, meaning that the WPT and communication will each have defined slots in time where only one is allowed to be operational. The implications of such a solution are discussed later in this thesis.

Neither WPT with inductive coupling nor NFC is a new research area. However, the coexistence of a dual WPT system with this specific setup is yet to be fully characterized. Therefore, this thesis will focus on the theoretical and practical integration of these coexisting systems.

A complete setup comprising a control system and coils to it are used to perform this study. Custom coils are built and characterized merely for this purpose. A filter and shielding have been implemented to attenuate interference between the

high-power and the communication coils. Shielding, in this case, implies enclosing sensitive parts of the communication system within a metallic cage. These two implementations were expected to ensure coexistence between the systems. However, the coexistence issue is still present with the mentioned implementations. Further investigations are needed to achieve coexistence between the high-power and communication systems.

Acknowledgments

Lund. Thank you for these years; there is no place like you. I have experienced many happy moments that I will not forget. I still remember the first time I arrived at the campus on an early summer morning some years ago. It doesn't seem long ago; I guess time moves fast when you have fun.

It has been a true pleasure to be at nok9 during my time as a Master thesis student. Every day came with new challenges, and never were two days the same. I am grateful for being part of the nok9 team. I am thankful for the brilliant people at nok9 that have helped me along the way. Professor Lau, Laurens, and Max, I have learned so much from you, and I will always be thankful for that. I also would like to thank Tomas Avramovic for always keeping me supplied.

Lastly, I thank my friends and family for making every day great!

Table of Contents

List of Figures

List of Tables

Acronyms

AM	Amplitude Modulation
BST	Base Station Tester
dB	Decibel
dBm	Decibel-milliwatt
DUT	Device Under Test
EM	Electromagnetic
ESR	Equivalent Series Resistance
EVA	Evaluation Tool
emf	Electromotive Force
FW	Firmware
GUI	Graphical User Interface
HF	High Frequency
Ki	Cordless Kitchen Standard
LC	Inductor and Capacitor
LF	Low Frequency
MDT	Mobile Device Tester
NFC	Near Field Communication
OOK	On-Off-Keying
PA	Power Amplifier
SA	Spectrum Analyzer
SE	Shielding Effectiveness
S Parameter	Scattering Parameter
SRF	Self Resonance Frequency
ST	STMicroelectronics
VNA	Vector Network Analyzer
WPT	Wireless Power Transfer
WPC	Wireless Power Consortium
2PN	2-Port Network

Symbols

A	Absorption
$\overline{B}$	Magnetic flux density
B	Re-reflection
$\overline{E}$	Electric field strength
$\mathrm{E_I}$	Incident wave
$\mathrm{E_R}$	Reflected wave
$\mathrm{E_B}$	Re-reflected wave
$\mathrm{E_T}$	Transmitted wave
F	Frequency
f_c	Cut-off frequency
$\overline{H}$	Magnetic field strength
$\overline{M}$	Magnetization
R	Reflection
r	Distance between shield barrier and source (in meters)
t	Thickness of barrier (in meters)
$\mathbf{Y}$	Admittance matrix
$\mathbf{Z}$	Impedance matrix
Z_0	Characteristic impedance
ϕ	Magnetic flux
σ	Conductivity
σ_r	Relative conductivity
δ	Skin depth
μ	Permeability
μ_0	Permeability of free space
μ_r	Relative permeability

Chapter 1
Introduction

1.1 Background

The idea of controlled power transfer through air is a concept coined over a century ago. Great scientists have, throughout the history, laid the foundation on which this thesis is based. Already in 1865, Scottish mathematician James Clerk Maxwell published a paper on the theory of electromagnetic fields. Although not experimentally confirmed at this time, Maxwell captures very well the philosophical aspects of the, for mankind's naked eye, invisible fields and forces constantly present in our world: electromagnetism [1]. His theories were later that decade confirmed by Heinrich Hertz [2]. A set of equations, now referred to as "Maxwells Equations", set up mainly by a trio called "The Maxwellians", made the theory practically applicable [3].

The Serbian scientist Nikola Tesla was a major contributor to the practical applications of these findings. At the end of the 1800s, Tesla introduced the concept of alternating electrical current (AC). He experimented with a transformer known as the "Tesla Coil" which produced electric fields strong enough to create light arcs. The idea of, as we call it today, wireless power transfer (WPT) was born with Tesla's successful experiments. In 1893 Tesla held lectures in the US where he, for the first time, publicly demonstrated an electrical apparatus referred to as a system for "transmitting intelligence, or perhaps power, to any distance through the earth or environing medium.". In other words, a system that would inductively couple two physically separated devices through air, and thus transferring energy between the two devices[1]. Already at this point, he talked about the importance of tuning the receiver and transmitter circuits [4], which we today know is highly important for the efficient transfer of power. These findings are now well over a century old, and today the world is running on wireless communication and, in a sense, wireless power transfer.

Nevertheless, electromagnetism is a complex subject of study and progress cannot be made overnight. Only in the most recent years has WPT started to become available for the public by means of charging mobile devices. The dominant standard for mobile phone charging, called Qi, was created by Wireless Power

[1] WPT and intelligence/communication over air through electromagnetism (EM) are two technologies utilizing the same concepts but are not identical in the sense on how they are implemented practically.

Consortium (WPC). The maturing of this technology has paved the path for yet more application areas, and kitchen appliances are one of those. At the beginning of the last decade, the WPC started creating a standard for WPT within the kitchen eco-system called Ki. The core goal of the standard is to achieve complete interoperability between all receivers (appliances) and transmitters (hobs). However, there have been several technical issues that have required time to resolve. Much of the knowledge and experience from the Qi technology is applied to the Ki standard. However, new technical challenges have appeared with the big step of raising the transferred power from tens of watts to 2200 watts.

1.2 Motivation

In contrast to the Qi standard, where WPT and communication are performed in-band, i.e., the same coils and frequencies are used for WPT and communication, the Ki standard which is currently being finalized, separates the physical link between WPT and communication. The WPT operates at around 30 kHz, whereas the communication, which adapts the NFC (Near Field Communication) standard, operates at 13.56 MHz. The WPT and communication links are physically separated using two sets of inductive coils (one transmit-receive coil pair for each band). However, with space limitations, the coils used for the different links are coupled inductively, meaning that there can be issues relating to coexistence of the WPT and communication systems. The realization of this coexistence is crucial for a safe and efficient system. The coils used for WPT, called the main coils henceforth, may be subjected to AC currents of up to tens of amperes, and should therefore be constructed in a safe way. As a consequence of unintended inductive coupling, so should the coils used for communication, called NFC coils henceforth, be designed carefully, as high level of currents may be induced otherwise. There is thus a need to decouple the main coil circuitry and the NFC coil circuitry to prevent destructively large currents as well as distortions of the communication signals in the NFC coils. In addition, the loading on the main coils due to the unwanted coupling to the NFC coils could also affect the efficiency of the WPT operation in the main coils.

Another technical challenge in the WPT operation of kitchen appliances is to enable low-power electronics in the appliance. Modern appliances have an onboard microcontroller to enable a user interface. It is desirable to have the user interface either in active or standby mode when the appliance itself is in an idle state. The main coils are built for power operation in the kilowatts range and are unsuitable for power electronics that require only a few watts or even less. Therefore, an attractive alternative is to use the NFC coils to also power the low-power electronics, apart from handling Ki communication. In 2020, the NFC Forum released a wireless charging specification with a power transfer rate of one watt [5], meaning that using the NFC interface for WPT is not a new technique. The coexistence of a Ki WPT system and an NFC communication system is the novelty of this implementation.

1.3 Goals

This thesis takes a pragmatic approach to address the two technical challenges identified above. Specifically, the proposed Ki system that incorporates main and NFC coils for WPT and communication will be built to enable the study of coexistence between the main coils and NFC coils, with the former dedicated to high power WPT and the latter used for both low-power WPT and communication. The goals are defined as follows:

- Achieve true coexistence between the main and NFC coils by means of circuit design. Verification of goal is done with a physical prototype.
- Design and build prototype to energize low-power electronics via the NFC coils, while ensure coexistence with the main coils and their WPT operation. Achieve a minimum guaranteed power of 500 mW.

One way of achieving the first goal is to decouple the main coils and NFC coils in time by introducing slotted communication, meaning that they will never be active simultaneously [6]. One compromise of this solution is the rate of data transfer since the communication channel, i.e., the NFC coils, will have to be constrained to time slots in which communication is allowed. This solution entails other complications such as lower maximum power that can be transferred during WPT, synchronization in the transmitter between the main and NFC coils, possible failure should the WPT and communication accidentally overlap, and increased protocol complexity. In the ideal case, the main coils and NFC coils would coexist in both time and space without any complication, which would be true coexistence. That would mean designing a system where WPT is active simultaneously as communication is performed, without any interference between the two. It would simplify the system in terms of protocol, remove the risk of dangerous levels of currents induced in the NFC coils, simplify the appliance electronics, and increase the possible data transfer rate. Given the different operation bands of main coils and NFC coils, this would imply implementing appropriate analog circuit filtering of the power and communication signals.

A power transfer link in the NFC channel will be established to fulfill the second goal. The magnitude of power of interest is low enough so that the NFC coils, typically used only for communication, may also be used for low-power WPT, just as in Qi. The challenge of enabling sufficient energy harvesting in the appliance through the NFC link will be to ensure that any combination of transmitters and kitchen appliances will satisfy this requirement. There will be many types of appliances produced by various manufacturers which all will be electronically different.

1.4 Structure of Thesis

Following this introductory chapter, a theoretical chapter will introduce the reader to relevant physical concepts such as electromagnetic fields, shielding of such fields, and circuit theory. This chapter may be helpful to understand what is written in the following chapters. Next, the characterization of the system will be a separate

chapter (i.e., Chapter 3) since this part turned out to be critical for designing a functional system. The characterization was chronologically done in parallel with the next chapter (Chapter 4), which is on implementation. These two chapters contain much of the results that have been achieved, and thus the results will not be presented in a separate chapter. The discussion is in Chapter 5. Finally, the conclusions and future work are presented in Chapter 6.

Chapter 2
Theoretical Background

Inductive WPT is a technology in which a transmitter device generates a magnetic field to which a receiver device is receptive by means of receiving and converting that magnetic field to electric power. The magnitude of the magnetic field the receiver may tap into will directly relate to how efficient the transfer will be. By adding additional circuitry to the devices, the WPT will be tuned to specific operating points decided by the designer.

2.1 Material Science

With the core science of WPT being rooted in the realm of one of the four fundamental forces: electromagnetism, the materials used to produce this force will be described in this section. When designing a WPT system today, the choice of material for the inductor is seldom considered since copper is the de facto standard. Isolated Litz wire made of copper is available on the market with any configuration the designer may wish to use. As a metal, copper has good conductivity at room temperatures, is ductile, and is cost-efficient compared to other metals with similar conductivity. In addition, copper is not ferromagnetic due to its electronic structure; the $3d$ energy level is completely filled [7]. The transition metals do not fill the shells paired since this is not energetically favorable. Instead, as electrons are added, they add to the same spin until the shells are half-filled. Exceptional cases occur, as for copper, which tends to favor an unfilled $4s$ shell rather than a $3d$ shell and thus showing no net magnetic moment. This is favorable since, in practical applications, the transmitter device and receiver device will not attract nor repel each other in an uncontrolled way.

To amplify the imposed magnetic field, generated in the transmitter device, towards a desired direction, a group of materials called ferrites is widely used [8]. A ferrite is a ceramic material with ferrimagnetic properties. A ceramic is an inorganic material with usually poor electrical conductive properties and good thermal insulation. This implies low losses through eddy currents, which is described in Section 2.2.2.

A ferrimagnetic material may be defined as a material with two or more ions with different magnetic moments. When imposed to a magnetic field, the ions will either line up with the field or oppose it. In the case of ferrimagnetic materials, the dipoles will not be equal, and thus a net magnetization is achieved [7]. This is

related to a property called magnetic permeability μ. If the net magnetic moment in the material aligns with the field and thus amplifies the field, the permeability of that material is higher than that of free space. In other words, permeability may be described as how concentrated a magnetic field is within a material, compared to the case of free air. The magnetic flux density ($\overline{\mathrm{B}}$) will then be related to the permeability and the magnetic field intensity ($\overline{\mathrm{H}}$) by the following equation:

$$\overline{\mathrm{B}} = \mu\overline{\mathrm{H}} = \mu_0\overline{\mathrm{H}} + \mu_0\overline{\mathrm{M}} \tag{2.1}$$

where $\overline{\mathrm{M}}$ is called the magnetization and represents the presence of a "magnetic" material. Similar to the fact that stress causes strain in any material, a magnetic field causes magnetization.

The microstructure of ferrimagnetics is based on domains in which all magnetic dipoles align. Between these domains, a thin wall called the Bloch wall is formed [7]. Inside this about 100 nm thin wall, the magnetic moment gradually changes from the direction of its one neighboring domain to the other. When an imposed field on a ferrite is removed, the Bloch wall will act as a resistance, hindering the domains from again converging to the virgin state of the material, thus leaving it in a permanently changed state with a residual magnetization known as the remanence [7].

The choice of ferrite is not trivial as there are numerous different shapes, materials, and desired electrical properties to consider. In addition, ferrites possess rather wide tolerances of their properties, and thus the frequency response of two ferrites with the same material may vary.

2.2 Electromagnetism

2.2.1 Origin of Magnetism

All materials are magnetic per definition, and it is due to the nature of the atom [7]. Magnetism is part of one of the fundamental forces, namely electromagnetism. In analogy to an electric current running through a closed circuit, the orbital and spin motions of the electron contribute to the magnetic behavior of a material. The spin will produce a magnetic field with a certain magnitude and direction at a given point in space. At the same time, the orbital motion creates a magnetic field surrounding the nucleus with which the electron is currently associated. In a sense, the electron may be thought of as a magnet itself. A magnet is realized when all electrons align and spin to produce a net moment in the same direction. Thanks to the Pauli exclusion principle, this will only be possible when certain electron shells are partly filled; thus, most elements will not be subject to a net magnetic moment. The most common element with a strong net magnetic moment is iron, which has four partly filled orbitals in the $3d$ energy level; it is widespread to have in ferrites [7]. The nature of magnetism is complex, and the theory could be explained indefinitely. To the naked eye of mankind, most of the electromagnetic (EM) spectrum is completely invisible [9]. Between Gamma rays with a wavelength shorter than a nanometer and radio waves with kilometer-long wavelengths, visible light is a tiny fraction of the EM spectrum spanning merely 300 nm

in wavelength. We may believe the world is objective as we see it, but in reality, it is not. The EM spectrum studied in this thesis is outside of the visible range; hence imagination and visualization play an important role in understanding the magnetic phenomenon.

2.2.2 Magnetic Fields and Induction

Magnetic fields can, in contrast to electric fields, be interpreted as a relativistic effect [10]. In an electric field, electrons will experience a disturbance of equilibrium and strive to reach equilibrium through the principles of thermodynamics. A magnetic field is, however, not something electrons will experience in that sense. Michael Faraday discovered in the early 1800s the electromotive force, which may be described as [11]

> "a time-varying magnetic field produces an *electromotive force* (emf) which may establish a current in a suitable close circuit. An electromotive force is merely a voltage that arises from conductors moving in a magnetic field or from changing magnetic fields"

Faraday defined an equation to describe this effect

$$\text{emf} = -\frac{d\Phi}{dt} \quad \text{(V)}, \tag{2.2}$$

which is today called Faraday's law of induction. Φ is the net magnetic flux [12]. The negative sign originates from the nature of how the induced current is directed, which German-born physicist Emil Lenz described in 1834. The physical meaning of this equation is that whenever $d\Phi/dt$ in a closed surface in space is nonzero, an adjacent conductive body will be subject to induction according to the law stated above. This situation may arise from either relative motion between the origin of the magnetic flux and the adjacent body or a time-changing flux of the origin. To point out the implication of the negative sign in Equation 2.2, an incident magnetic wave will induce a voltage in a body of such a direction that the resulting currents will itself radiate a reflected magnetic wave of the opposite phase, relative to that of the incident wave; so to counteract the incident wave.

2.2.3 Eddy Currents

When a conducting body is exposed to an alternating current (AC), EM fields will be created around this body. If now a second conducting body is placed near the first body, currents called "Eddy Currents" will be induced by these EM fields, as predicted by Faraday [13]. The currents will form loops so to comply with Lenz's law. One effect of Eddy currents is ohmic losses called induction heating, which is used for cooking in modern kitchens [14]. Another significant effect is the force between the incident magnetic wave and the reflected wave produced by the Eddy currents. This will manifest itself as a change in impedance seen at the source—a conducting body in proximity to another conducting body will effectively impact the impedance of the former. To understand from a different perspective of how the resistance in a coil can change merely due to the presence of a conducting

body, the first law of thermodynamics may be thought of as: the total energy of an isolated system is constant. Imagine a volume in space in which both a fictive coil and a conducing body is present. Assume that an AC current is applied to the coil and that the magnetic flux from the coil penetrates that body. Eddy currents will cause the body to heat up: energy is consumed. The source of that consumed energy is manifested in the coil as increased resistance. This is commonly called self-resistance [15].

It should be noted that, in a practical transformer, Eddy currents may be induced on the secondary side, even in the case of an open circuit.

2.2.4 Self and Mutual Impedance

The change in self-resistance described above is accompanied by a change in reactance. In addition to real losses, there is a reactive effect that origins from Faraday's law, as described above [11]. Assume a time-varying current in a transformer. Then the primary inductor emits a magnetic field which induces a voltage onto itself; self-inductance. If we now include the effects of the secondary inductor, the magnetic flux from the primary side will produce an emf in the secondary side as well; mutual inductance. In other words, mutual inductance, similar to self-resistance, arises with a magnetic field being affected by the sole presence of an electrically permeable medium within the space in which that magnetic field exists.

Mutual inductance is part of the mutual impedance, implying that a mutual resistance exists. The mutual resistance may be explained in the transformer's case again. Assume a driving signal is applied on both the primary and secondary sides. Each inductor will generate a magnetic field that will impact the other inductor. As superposition applies, the interaction between these two driving fields will cause additional changes in losses on both sides: mutual resistance. More on the practical implications of this can be read in [16].

2.3 Network Analysis

In the Ki and Qi standards, the operating frequency of the main WPT signal is in the range of a maximum of a few hundred kHz [17]. Accurate measurements at these frequencies are traditionally associated with LCR meters or similar tools, which use the lumped element measurement method. The NFC coils, which operate at 13.56 MHz, have a wavelength of about 22 m, indicating that the lumped element method may still be a good model. However, a distributed element model may provide more insight into the system, as the tools utilizing this model can provide multiple-port measurements. The vector network analyzer (VNA) is a tool developed during the second half of the 1900s to determine passive components' scattering parameters (S Parameters) [18]. The VNA was born mainly to measure impedance at frequencies where the wavelength is of similar size or smaller than the devices being measured. One of the main differences between a VNA and an LCR meter is that the VNA can separate an incident wave from a reflected wave, which is described below.

2.3.1 Wave Quantities

Before describing the S parameters, the concept of wave quantities will be introduced. Imagine an alternating voltage source generating an alternating current within a circuit: an EM wave is generated. This wave will have a specific impedance called the wave impedance, characterized by the relation between the electric field and the magnetic field. Far away from the source, that relation is constant, and the wave is known as a plane wave [19]. However, close to the source, that relation will be determined by the circuit properties. As electric fields (E-fields) arise with an imbalance of charge, a significant voltage difference in the circuit will generate a predominant electric field. Magnetic fields (H-fields) arise with current changes in the circuit. The wave impedance is $Z_0 = E/H$. The circuits studied in this thesis are loops exclusively; H-fields will dominate, and the wave impedance will be very low. When the propagating wave encounters a medium with a different impedance to the wave, part of that wave will propagate into that medium; and part of it will reflect towards the impinging wave [19]. Why this occurs may be described with the help of optics, where Dutch physicist Christiaan Huygens at the end of the 1600s, discovered this behaviour [20]. A wave with a fixed frequency propagates through space in a medium with a specific wave impedance. It will have a speed determined by the medium it propagates through—light propagating in the air is one such example. When the wave encounters a different medium with different properties, the speed of the wave will change; refraction occurs. One effect of refraction is that the direction of propagation will be bent. The interface between air and water is a visible example that shows all these effects.

It should be noted that, although created in different processes, visible light and the EM waves studied in this thesis originate from the same fundamental force: electromagnetism. The word photon is Greek for light and is used to describe visible light, whereas EM waves are not usually associated with that term. The quantum mechanics wave-particle duality theory will be more relevant for the short wavelength of visible light. However, effects due to the wave-like behavior of light may be used in analogy to explain certain behavior of the EM waves.

2.3.2 S Parameters

The VNA uses the theory of waves to compute the characteristics of an n-port system, where n is the number of ports of the system to compute the S parameters. Assume a 2-port device under test (DUT) as in Figure 2.1.

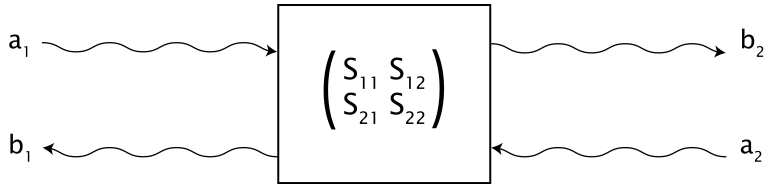

Figure 2.1: 2-port network described with waves.

Each port of the VNA has a current generator with a known source resistance, usually 50 Ohm, along with a receiver circuit. The working principle is to stimulate the DUT from one port at a time and measure both the transmitted and reflected waves by means of amplitude and phase. In contrast to an LCR meter, the VNA is able to separate the transmitted and reflected waves by using couplers or bridges. The measured parameters are, in fact, a complex voltage that relates to the S parameters as follows

$$\begin{pmatrix} b_1 \\ \vdots \\ b_n \end{pmatrix} = \begin{pmatrix} S_{11} & \dots & S_{1n} \\ \vdots & \ddots & \vdots \\ S_{n1} & \dots & S_{nn} \end{pmatrix} \begin{pmatrix} a_1 \\ \vdots \\ a_n \end{pmatrix}, \tag{2.3}$$

with the complex parameters a and b being the wave quantities as in Figure 2.1. The wave quantities a_i and b_i are calculated from the measured complex voltage divided by the known source impedance[1]. The S parameters for a two port network are then calculated from the wave ratios of a_i and b_i under the following conditions

$$S_{11} = \left.\frac{b_1}{a_1}\right|_{a_2=0}, \tag{2.4}$$

$$S_{12} = \left.\frac{b_1}{a_2}\right|_{a_1=0}, \tag{2.5}$$

$$S_{21} = \left.\frac{b_2}{a_1}\right|_{a_2=0}, \tag{2.6}$$

$$S_{22} = \left.\frac{b_2}{a_2}\right|_{a_1=0}. \tag{2.7}$$

S_{21} is usually referred to as the insertion loss and is useful for the determination of how much power is transferred through a DUT when the load matches the source impedance. The condition $|_{a_2=0}$ means that port two is terminated with, in this case, 50 Ohm, and no driving signal is applied on that port.

2.3.3 Network Conversions

The S parameters are rather general, and there are other ways of describing a network. To characterize a DUT in terms of impedance or any other desired form, the S parameters may be converted [21]. To obtain the impedance matrix ($\mathbf{Z}$), the following equation is used for the two port network

$$\mathbf{Z} = \frac{Z_0}{\Delta S} \begin{pmatrix} (1+S_{11})(1+S_{22}) - S_{12}S_{21} & 2S_{12} \\ 2S_{12} & (1-S_{11})(1+S_{22}) + S_{12}S_{21} \end{pmatrix}, \tag{2.8}$$

[1]Note that the unit of a_i and b_i is $\sqrt{\text{power}}$.

where $\Delta S = (1 - S_{11})(1 - S_{22}) - S_{12}S_{21}$. The Z-matrix, together with the admittance matrix ($\mathbf{Y}$=$\mathbf{Z}^{-1}$), is useful when investigating series and parallel resonance circuits within the DUT.

Obtaining complex gain from one port to another is one of the advantages of using a VNA as compared to an impedance analyzer or an LCR meter. This is because the phase information between the ports is known, and so the power transfer can be computed. This can be done in different ways, depending on the resources available. MATLAB has these functions implemented directly, and those will be used. Specifically, the voltage transfer function from the input voltage to the output voltage and the power transfer from the input power to output power will be of interest[2].

2.4 Shielding of Magnetic Fields

The NFC coils will be placed physically close to the main coils, and so will the circuitry of the two separate systems. The consequence is that the magnetic flux from the main coils will penetrate the NFC coils and their respective circuitry. One of the functions of the said circuitry is to insulate the main field from the NFC field. This is described in Section 2.5. However, if the circuitry is placed in a space where the flux fully or partly penetrates it from the main field, undesirable interference will still be induced, and coexistence is put at risk. To insulate the NFC circuitry from the present magnetic flux from the main coils, shielding, in the form of a barrier, will be incorporated into the practical design.

2.4.1 Shielding Theory

Assume an EM wave traveling in free air. At one point, the wave hits a barrier, as shown in Figure 2.2. Refer to Section 2.3.1 for the explanation of the physics that will cause the wave to partly transmit through the barrier and simultaneously reflect back towards the incident wave.

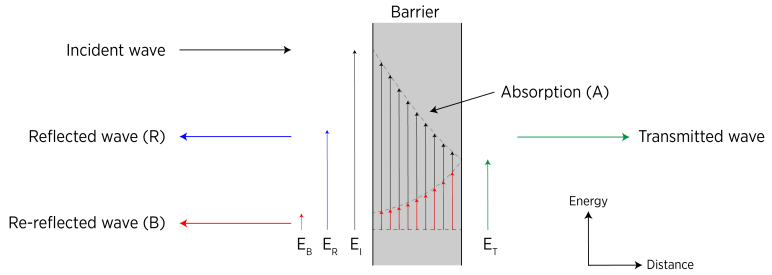

Figure 2.2: A barrier shield.

Shielding, in this case, refers to the ability to cancel out an incident wave so that the transmitted wave is minimized. There are four effects to consider when

[2]The gain functions are part of the MATLAB RF Toolbox and documented by MathWorks. The name of these functions are "s2tf" and "powergain" respectively.

optimizing for good shielding:

- Reflection (R)
- Absorption (A)
- Re-reflection (B)
- Flux Guiding

Reflection Loss

The reflection will depend on the ratio of wave impedance to the barrier impedance. Recall again from Section 2.3.1 that the wave impedance of fields generated by the main coils will be very low close to the source. The wavelength of the main field will be a few kilometers long, and thus we will always be in the near field of the source, i.e., close to the source. Two material properties determine the impedance of the barrier: conductivity σ and permeability μ. A material with high permeability will, in a sense, guide magnetic flux lines through itself. Due to the skin effect, the frequency will also impact the impedance. For predominant magnetic fields, the reflection loss $\mathrm{R_H}$ is defined as [19]

$$\mathrm{R_H} = 14.6 - 10\log_{10}((\mu_r/\sigma_r)/(\mathrm{F}\cdot\mathrm{r}^2))\ \mathrm{dB}, \tag{2.9}$$

where σ_r is the dimensionless relative conductivity and μ_r is the dimensionless relative permeability. Relative in this case means that it is in ratio to the conductivity and permeability of vacuum, respectively. F is the frequency of the field (in Hz), and r is the distance from the source in meters. Shielding will need to rely on the choice of material for the barrier: the material should possess high permeability rather than high conductivity. However, the mechanism of achieving effective shielding is not through reflection but flux guiding, as will be described later in this section.

Absorption Loss

Absorption is seen in Figure 2.2 as a decreasing signal strength when traveling through a material. This loss depends only on the thickness of the barrier t and the skin depth δ. The term skin depth is a property that describes how AC currents will be confined on the surface of a conducting material. It states that for each skin depth, an impinging signal will be attenuated 8.6 dB (1/e) in the material. The absorption A is defined as [19]

$$\mathrm{A} = 8.69\cdot(\mathrm{t}/\delta)\ \mathrm{dB}, \tag{2.10}$$

where t is the thickness in meters of the barrier, and the skin depth is defined as

$$\delta = \frac{1}{\sqrt{\pi\cdot\mathrm{F}\cdot\mu\cdot\sigma}}. \tag{2.11}$$

Re-reflection Loss

Multiple reflections will deteriorate the total shielding effectiveness but will, in most cases, be negligible. This is true if the barrier thickness is equal to or less than the skin depth [19]. For example, a 45 kHz field will have a skin depth of around 10 μm. It will not be considered further.

The convenience with the logarithmic scale is that the product of two linear values becomes a simple addition. Thus, the total shielding effectiveness (SE) becomes[3]

$$\mathrm{SE} = R + A \ (\mathrm{dB}). \tag{2.12}$$

Flux Guiding

Good shielding of low frequency (LF) magnetic fields depends on mechanisms that rely on the permeability of the material. LF, in this case, will be limited to some tens of kilohertz. The term reluctance may be introduced to describe this mechanism better. Reluctance is a measure of magnetic resistance, and it is inversely proportional to permeability: high permeability implies low reluctance. For example, assume an LF magnetic field in free air. If a body of iron is placed in this field, the flux will tend to bend towards and into this body to take the path with the lowest reluctance, as nature is always striving for the lower energy state. The introduced path will indeed mean a longer total path for the flux. However, if the total energy is lower by taking that path, it will still be the preferred path for the EM wave.

This means that a volume of sensitive content may be shielded from an external LF magnetic field by guiding the magnetic flux lines through a material surrounding the content.

2.5 Circuit Theory

2.5.1 Real Coils

A real coil, when translated to a circuit representation, will always carry parasitic elements, which will be significant when the frequency is high enough. This effect will be seen when the self-resonance frequency (SRF) of the coils is measured, the results of which will be presented in Section 3.1. The equivalent circuit of a real coil will look as in Figure 2.3. This circuit will resonate at specific frequencies depending on the magnitude of the inductance value and the parasitic capacitance C_P [19]. The resistance R in the coil will vary depending on the operating point, but it will only affect the damping of the system, and not the locus of the SRF.

[3]Note that the re-reflection (B) is neglected. For barriers which are thinner than one skin depth, this factor may be considered.

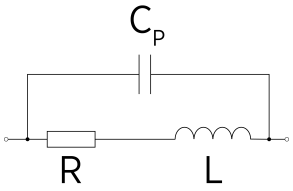

Figure 2.3: The equivalent circuit model of a real coil.

2.5.2 LC Circuits

There are two types of LC circuits: series- and parallel circuits. In Figure 2.4 these are shown. Such circuits will resonate at a specific angular frequency ω_0. In both cases, this frequency is defined as

$$\omega_0 = \frac{1}{\sqrt{\mathrm{LC}}} \tag{2.13}$$

where $\omega_0 = 2\pi f_0$. In the case of a parallel LC circuit, as in Figure 2.4 a), the impedance at resonance will become theoretically infinite. In the case of a series LC circuit, as in Figure 2.4 b), the resonance impedance is 0. These statements are proven in Appendix A.

At the point of the resonance, the phase of the circuit will make an abrupt 180-degree shift[4], thus changing its behavior. In the case of the parallel circuit, the phase will be +90 degrees below the resonance point, and thus showing an inductive behavior. However, after the resonance point, it will become capacitive, and the phase will become -90 degrees.

Measurements of the SRF due to parasitic elements may be performed with a VNA. The S-parameters is transformed into Z- and Y-parameters to obtain the parallel- and series self-resonance frequency, respectively. The inductance of the physical coil is also measured with the VNA by looking at the reactance of the Z-parameter at a frequency much lower than the locus of the parallel resonance. With both the SRF and inductance known, the parasitic elements can be calculated using Equation 2.13.

2.5.3 Decoupling of Main Coils and NFC Coils

The main coils will operate in the frequency region around 30 kHz, while the NFC coils will operate at around 13.56 MHz. To decouple the two, a filter circuit will be implemented. The NFC coils are physical inductors that, together with a physical capacitor, may form either a series- or parallel LC-filter as shown in Figure 2.4.

[4]The phase is defined as the instantaneous phase of the voltage minus the instantaneous phase of the current. A coil will oppose an initial current applied, and so the current will lag the voltage by 90 degrees. A capacitor will, on the other hand, take time to charge up due to the dielectric polarization of the material, thus showing a negative 90-degree shift.

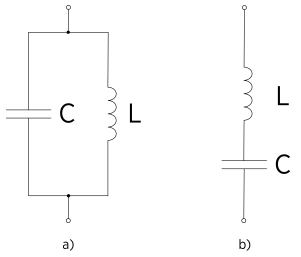

Figure 2.4: Two LC Filters. a) Parallel LC circuit. b) Series LC circuit.

This may be used to form a bandpass filter suitable for a frequency range of interest. In this case, the frequency for NFC operation. The parallel LC-filter is a 2nd order filter and will have a slope of 40 dB/decade. Higher order filter may be built, but as this will be a very simple and effective filter for this case it will be used initially.

It should be noted that a real inductor will have a parasitic parallel capacitance, forming a parallel LC resonance circuit. The parasitic capacitance is usually very low, and thus, the parasitic resonance frequency will be very high according to Equation 2.13.

2.6 Power Amplifier and Energy Harvesting

The purpose of the amplifier is to ensure that the kitchen appliance low-power electronics power needs is met. The aim is to provide minimum 500 mW of active power to the appliance, at all times. Since the receiving device will not be in a fixed position with regards to the transmitting device, all possible, or at least all representative, positions should be considered when designing the amplifier. The power amplifier will be added to the NFC transmitting circuitry, and the energy harvester on the NFC receiving circuitry.

Chapter 3

System Characterization

The system comprises four coils and circuitry thereto[1]. The electromechanical properties of this entire system will be characterized in order to design proper filtering circuits to accomplish the coexistence goal. The coils were built after mechanical restrictions[2], rather than electrical, and so the coils will be the starting point at which the rest of the circuitry will be designed after. The two main coils, i.e., those that perform the high power transfer is seen in Figure 3.1. In such a configuration, the main Tx is said to be inductively coupled to the main Rx; they are mated.

Figure 3.1: Main Tx coil (bottom) mated with the main Rx coil (top).

The NFC coils are sandwiched between the two main coils, as seen in Figure 3.2. Now, there are four coils which are inductively mated to one another.

[1]The manufacturing of the coils are introduced first in Chapter 4, Section 4.4. The reader may refer to this section in parallel.

[2]The kitchen appliances will determine how big the two coils can be.

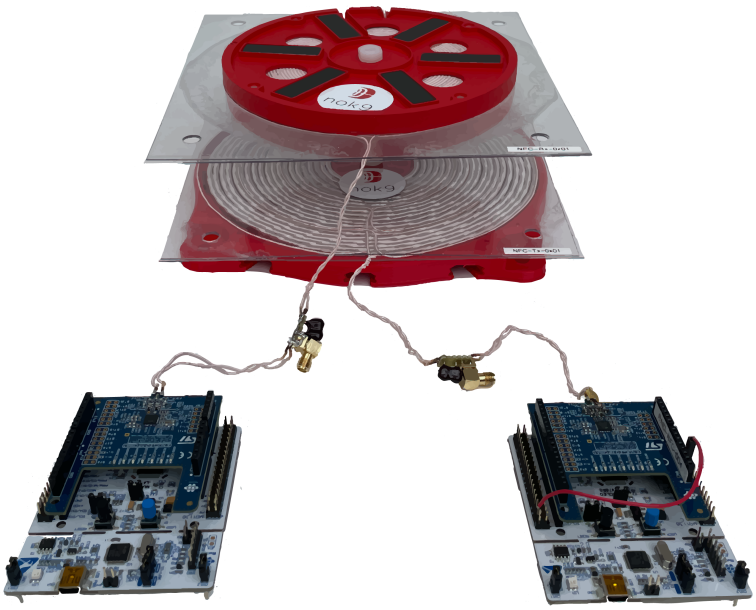

Figure 3.2: The NFC coils are located between the main coils. The NFC devices are seen in the bottom of the image.

3.1 Coil Setup

The coils and the Litz wire[3] used to build them, are defined in Table 3.1. It can be noted that the skin depth, using Equation 2.11, is about 300 and 18 μm in the main coils and NFC coils, respectively. This means that in the NFC coils, the current will be confined to the outer part of each conductor. By looking at the wire cross-section, it can be calculated that 59% of the cross-sectional wire area will contain current densities, which are damped by less than 8.6 dB (1/e).

Coil ID	Litz Wire	Windings	Layers	$\varnothing_{\text{inner}}$ /mm	$\varnothing_{\text{outer}}$ /mm
Ki-Tx-0x01	100/600	20	1	50	205
Ki-Rx-0x01	Unknown	22	2	62	148
NFC-Tx-0x01	100/60	3	1	21	11
NFC-Rx-0x01	100/60	2	1	17	17

Table 3.1: Mechanical definitions of the coils under investigation.

First, all the coils that is to be used will be characterized. This may be done in two different ways.

[3]The naming of Litz wire is defined as diameter in μm over the number of strands. 100/600 is a roughly 3.5 mm thick wire containing 600 wires that each are 100 μm in diameter.

- Isolated condition
- Mated condition

Either a VNA or an LCR meter can be used to measure the coils individually, one by one, i.e., not magnetically coupled to any of the other coils. The main Tx coil and NFC Tx coil of a unit will always be fixed to one another. However, the main Rx coil and NFC Rx coil may suddenly be removed and effectively changing the setup. But during WPT, they will be mated together. The characterization will be done with all coils mounted in that place and by performing measurements with a VNA since that will be the setup seen during WPT[4]. These two setups will yield outcomes parted from one another, as can be understood by reading Section 2.2.4. In addition to those effects described therein, the proximity effect[5] will effectively increase the resistance in all coils as they are mounted and complicate the design even further. The parasitic capacitance to surrounding metal objects will indeed also affect the SRF. The decision must be made whether the system is to be characterized in isolated or mated conditions. One could argue that the mated conditions will reflect the reality better. However, this implies that the characterization will only be valid for identical implementations like the one measured, which is not a good reflection of the reality; many kitchen appliances will have different implementations. Both isolated and mated conditions will be measured and compared.

3.2 Self Resonance Frequency | Comparison

The main coils were connected both in an isolated and mated state to the VNA. The connection between the VNA and the coils consists of cable lugs, as this will be the connector used in the real application. As expected, the increased parasitic capacitance does directly decrease the locus of the SRF; recall Equation 2.13. This is seen in Figure 3.3.

It can be seen that the simple equivalent circuit defined in Section 2.5 is a simplification; multiple resonance points indicate a significantly more complex circuit. The lowest SRF is still separable and it reflects the largest parallel capacitance of the circuit. The cable lugs used to connect the coils to the VNA have been seen to introduce very poor measurements at higher frequencies, which would be expected. But at the LF, where the main coils operate, there have not been any significant variations between measurements with cable lugs and with SMA directly soldered on the coil Litz wire. The effect of the cable lugs is seen when measuring the NFC coils at HF. As shown in Figure 3.4, the bare coils are measured isolated with the cable lugs as the connection between coil and VNA.

The isolated condition should only consist of a single resonance: the SRF, which is determined by the parasitic parallel capacitor. This is clearly not the

[4]The NFC Tx coil may be used to detect whenever an Rx device is present, and thus that configuration may also be investigated.

[5]The proximity effect may be categorized as a type of Eddy current. Similar to the skin depth, it will decrease the effective area of current flow in a conductor and thus increase the resistance of that conductor [22].

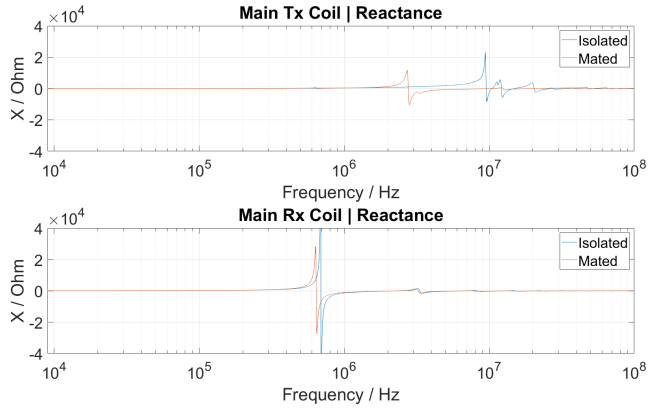

Figure 3.3: Coil reactance. Identification of a SRF is done by searching for the point where the reactance is 0.

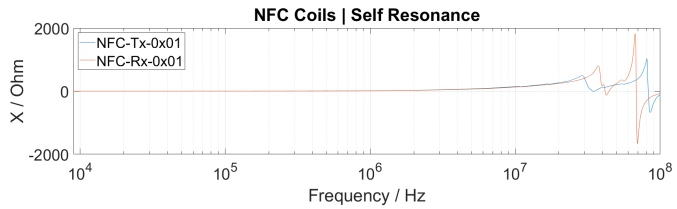

Figure 3.4: Self resonance of the NFC coils, when cable lugs are used as connection.

case, and so the cable lugs are replaced by an experiment board on which both the coil Litz wire and an SMA connector are soldered onto. The effect of this is seen in Figure 3.5.

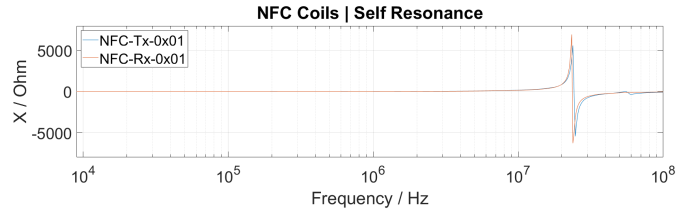

Figure 3.5: Self resonance of the NFC coils, when SMA is used as connection.

It is clear that the cable lugs cause false measurements at HF. Those measurements will be neglected, and cable lugs will only be used for LF measurements.

3.3 LC Filter

The filter that will be described in Chapter 4, Section 4.5 was then added to the NFC coils and the coil system was measured again in air. Note that the filter design and system characterization are done in parallel, but the design of the filter is introduced first in Chapter 4. As the idea is to have the filter attached during operation, the characterization was made with those included. Now we will study the phase of the impedance to see that the assembly is still inductive at the desired frequencies. Of the bare NFC coils, the phase is +90 degrees up until the SRF, where it changes to -90 degrees and becomes capacitive. With the filter included, the circuits will be capacitive up until the resonance frequency of the parallel LC filter[6] where it will make a switch from -90 to +90 degrees. The behavior at the SRF is still expected; thus, an inductive shed is created between the filter resonance and the SRF. This is very clearly visualized in Figure 3.6. Note that the increase in phase in the bottom graph of Figure 3.6 for low frequencies is due to the fact that the series capacitor will not allow any signal passing; the VNA cannot measure the phase if there is no signal to measure on.

The next step was to do the same measurement when the NFC coils were placed at their designated location where the main coils and other high-permeable materials surrounded them. It was clear that there is a difference between the isolated and mated conditions when observing the results in Figure 3.3. The NFC coils need to be inductive when mounted in EVA III MDT[7]. Both main coils were present, and both were left open circuit. The result is seen in Figure 3.7.

It is clear that the beautiful inductive region between 10 MHz and 24 MHz is not the case in reality. Figure 3.6 and Figure 3.7 confirm a very important part of

[6]Refer to Section 4.5 for the design of the filter.

[7]EVA III MDT is the tool used to evaluate the WPT. The tool is introduced and described in Chapter 4.

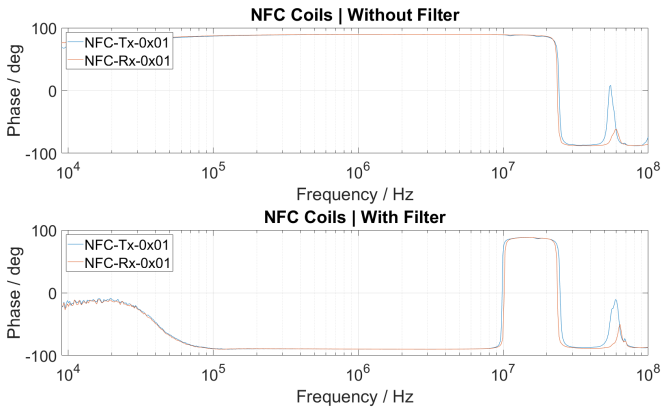

Figure 3.6: The phase of the NFC coils with and without the LC filter in air.

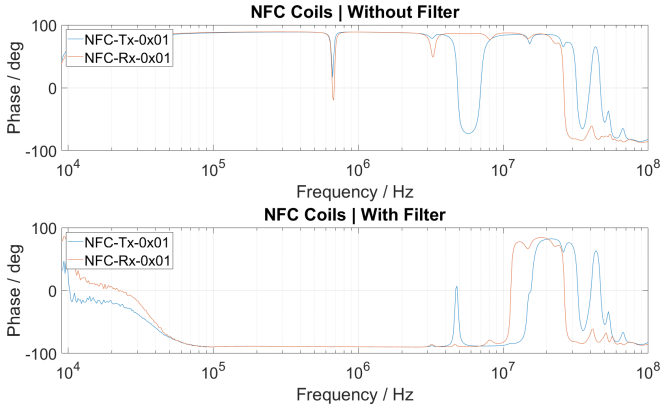

Figure 3.7: The phase of the NFC coils with and without the LC filter when mounted in EVA III MDT.

electronics: the importance of correct measurements. NFC-Tx-0x01 needs to be changed to be inductive at 13.56 MHz. A simple change would be to increase the value of the capacitor. This would decrease the resonance point of the LC filter. The series capacitor was increased from 100 pF to 200 pF[8], and the result is seen in Figure 3.8.

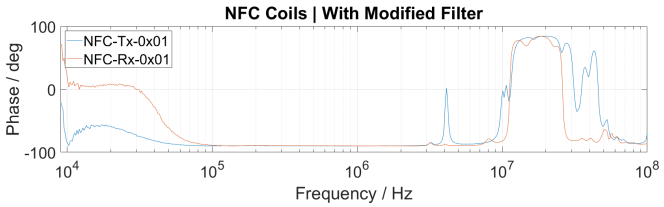

Figure 3.8: Modifying the filter of the NFC-Tx-0x01 to decrease the resonance frequency.

The above measurements were done with the VNA, and thus any circuit parameter may be extracted from the S parameters. The inductance of each coil was naturally measured without the filter and far below the SRF, where it is constant. The equivalent circuit of each coil can also be determined. The electrical properties of the coils are seen in Table 3.2. C_P is the parasitic parallel capacitance as introduced in Figure 2.3.

	Isolated Condition			Mated Condition		
Coil ID	L /μH	C_P /pF	SRF /MHz	L /μH	C_P /pF	SRF /MHz
Ki-Tx-0x01	59.3	4.8	9.4	57.6	57.7	2.8
Ki-Rx-0x01	278.0	191.3	0.7	280	220.9	0.6
NFC-Tx-0x01	2.5	17.0	24.2	2.5	20.0	32.0
NFC-Rx-0x01	2.2	19.5	24.0	2.2	17.0	26.0

Table 3.2: Electrical properties of the coils, isolated and mated. Without filter.

When measuring the NFC coils in the mated condition, the main coils in Table 3.2 were left open circuit. If those were shorted, the result would be rather different. The main coils were shorted, one at a time, and the result of the NFC coils is seen in Table 3.3. It can be seen that the inductance of the NFC Tx coil decreases significantly when the adjacent main coil is short-circuited.

[8] Again, recall that the filter design is introduced further down in Section 4.5.

Main Tx : Rx	Short : Short	Short : Open	Open : Short	Open : Open
Coil ID	L /μH	L /μH	L /μH	L / μH
NFC-Tx-0x01	1.3	1.2	2.4	2.6
NFC-Rx-0x01	1.9	2.0	1.9	2.2

Table 3.3: Inductance of NFC coils when main coils were open or short circuited.

The cases in Table 3.3 are the corner cases. In operation, the main coil termination will be different but somewhere between those cases. The equivalent series resistance (ESR) of the coils was also measured but at specific operating points. Those are found in Table 3.4. The main coils are open-circuited for the data regarding the NFC coils in Table 3.4.

	Isolated Condition		Mated Condition	
Operating Frequency	45 kHz	13.56 MHz	45 kHz	13.56 MHz
Coil ID	R /mΩ	R /Ω	R /mΩ	R /Ω
Ki-Tx-0x01	40	Unknown	70	138.0
Ki-Rx-0x01	330	Unknown	350	147.0
NFC-Tx-0x01	80	6.86	70	8.48
NFC-Rx-0x01	60	5.65	50	17.43

Table 3.4: Coil ESR for LF and HF, isolated and mated.

As expected, the self-resistance increases when there were objects near the coil under measurement. At 45 kHz, the resistance does not change significantly, going from the isolated to the mated condition; the 10 mΩ difference is most likely due to measurement uncertainty. Refer to Chapter 2, Section 2.2.3 for the explanation of this behavior.

3.4 Transfer Function

By using the collected data from the mated setup, the transfer function from the NFC Tx coil to the NFC Rx coil can be computed using the functions implemented in MATLAB as introduced in Section 2.3.3. The voltage transfer, with the LC filter included, is seen in Figure 3.9.

This can be compared with the active power gain that is seen below in Figure 3.10.

It is clear that the transfer bandwidth is very narrow at the point of operation. Another factor that contributes to the amount power transferred is the coupling factor k, which is a measure of how much of the magnetic field the receiver taps from the transmitter. k is defined as

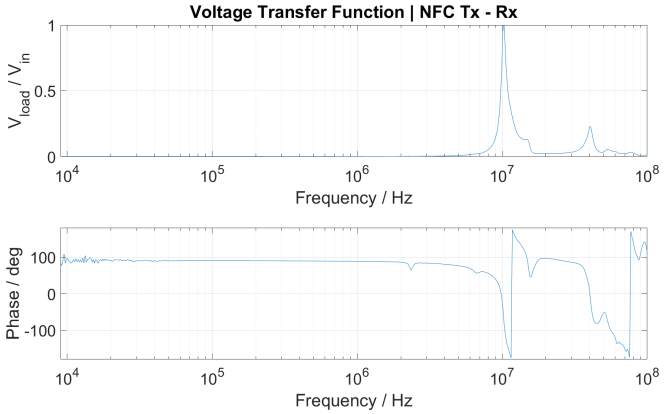

Figure 3.9: Magnitude (top) and phase (bottom) of the voltage transfer function from NFC-Tx-0x01 to NFC-Rx-0x01.

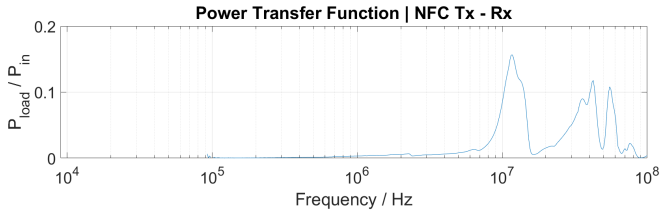

Figure 3.10: Magnitude of the power transfer function from NFC-Tx-0x01 to NFC-Rx-0x01. Note that this is active power, i.e., the power that is dissipated in the load.

$$k = \frac{\mathrm{Im}(Z_{12})}{\sqrt{\mathrm{Im}(Z_{11}) \cdot \mathrm{Im}(Z_{22})}}, \tag{3.1}$$

where the transmitter is connected to port 1, and the receiver to port 2 of a 2-port network (2PN). It is a value defined between 0 and 1. This information is obtained from the S-parameters and k is plotted over frequency in Figure 3.11.

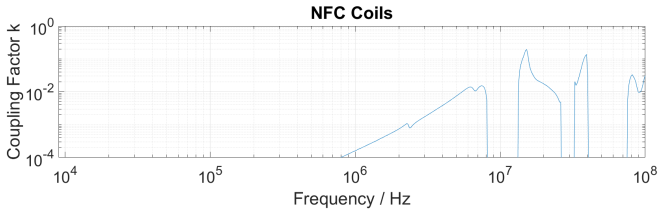

Figure 3.11: The coupling factor over frequency for the NFC coils when mounted in EVA III MDT.

It is seen that the coupling factor is rising fast at 13.56 MHz, implying that the configuration is somewhat optimum. The main Tx and main Rx are both shorted during the measurements.

Chapter 4
Implementation

The thesis of coexistence will, after circuit simulations, be tested directly on a physical WPT system. Such a system will comprise the following components.

- Transmitting main coil and a control system of it.
- Receiving main coil in the form of a water kettle.
- Transmitting and receiving NFC coils and control systems of those.

The transmitting coil and its associated control system were constructed at nok9. These belong to a larger system called EVA III, which includes two units: a mobile device tester (MDT) and a base station tester (BST). Only the MDT, which is an evaluation tool for power receivers that allows up to 2.5 kW of WPT, will be used. Together with a water kettle, modified by Philips to act as the receiving main coil, the EVA III MDT is able to boil water through WPT. The NFC coils and their filtering circuitry were constructed at nok9. The control systems associated with the NFC coils were provided by STMicroelectronics (ST). ST also provided the Ki-specific firmware[1] for the control system.

4.1 Priority of Implementation

Some parts of the thesis rely on other parts, and thus to ensure that each step is done in a proper order, the priorities of implementation will be outlined. If time does not allow for all parts to be completed, or if some parts are not successfully implemented, the chances of having completed the most critical parts is higher, while the less important parts may be left for future work. The priorities are listed in Table 4.1.

[1]The standard NFC protocol is included with the units. However, there is a specific implementation for the NFC communication in Ki. This implementation has been done by ST. ST has agreed to share this implementation with nok9 in confidence.

Priority	Description	Motivation
1	EVA III MDT Assembly	To test the coexistence subject, EVA will be needed.
2	NFC Control System	To test the communication with our own NFC coils which will be fitted in EVA.
3	Coil Production	Winding of custom coils (both main and NFC) to be used in the setup.
4	Decoupling	Demonstrate successful communication with the NFC coils mounted in EVA.
5	Power Amplifier	For the purpose of sufficient power transfer for standby mode. The PA will not be needed for communication.
6	Energy Harvester	To receive and tap into the power from the PA.

Table 4.1: Implementation priorities.

4.2 EVA III MDT Assembly

EVA is a tool designed to evaluate kitchen appliances that seek to comply with Ki. During the experiments, it was used for the sole purpose of generating a magnetic field that intentionally interferes with the NFC coils. A complete system was assembled for the experiments. The assembly includes mostly mechanical work but also programming of the control system. EVA III MDT is a mechanical box made out of an aluminum frame. The CAD drawing of an EVA III MDT is shown in Figure 4.1. In the top part of the unit, the main Tx coil can be seen. The NFC Tx coil will be mounted directly on top of the main Tx coil (in a co-centred fashion), but it is not included in the image.

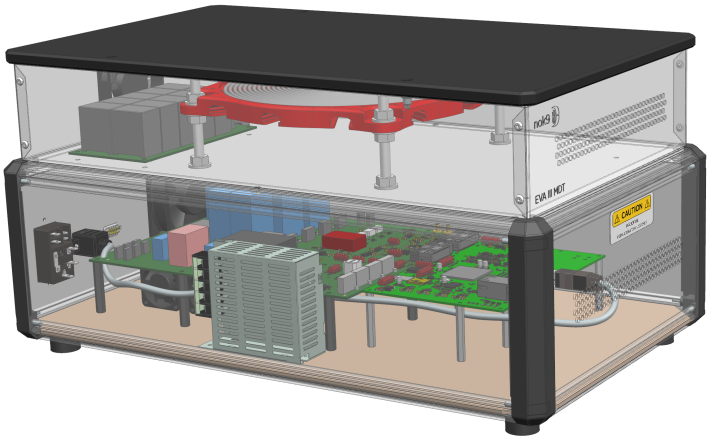

Figure 4.1: CAD of EVA III MDT.

The electronics to control the WPT are placed in the bottom part of the device. All electronics are designed by nok9. To control EVA, a USB interface is available, which can be connected to an external computer. A complete graphical user interface (GUI) built by nok9 lets the user control the device with ease.

4.3 NFC Control System

ST has been working on the implementation of the Ki-specific NFC communication and has provided nok9 with this implementation. The NFC hardware units used are named NUCLEO-L476RG and X-NUCLEO-NFC06A1, which are development boards used for regular NFC development. They will be connected together as the NUCLEO-L476RG, which contains an STM32L476 MCU, controls the NFC chip, ST25R3916, on the X-NUCLEO-NFC06A1 board. ST25R3916 is capable of being programmed as either a transmitter or receiver device. Thus, two identical devices will be used as the transmitter and receiver pair but programmed differently. A connected unit is seen in Figure 4.2. The NFC coil is seen to the right in that picture as three parallel white traces constituting a multi-turn loop. The NUCLEO-L476RG includes a debugger for easy programming and it does not need additional probes other than a mini-USB. To program the units, the software STM32CubeIDE is used.

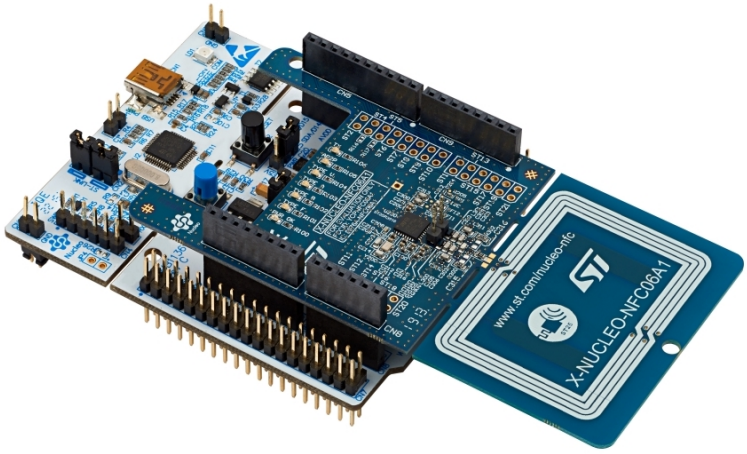

Figure 4.2: The NUCLEO-L476RG (bottom PCBA in white) mated with the X-NUCLEO-NFC06A1 (top PCBA in blue).

4.3.1 NFC Operation

The transmitter device communicates with the receiver device by utilizing On-Off-Keying (OOK). This means that during operation, the transmitter turns off the

driving signal so that the oscillation amplitude of the coil decays[2], for a certain amount of time before turning on the driving signal again. The receiver will be affected by this and can decode the modulated signal by recognizing patterns as defined by the NFC protocol, which will then be translated to packets of data containing information. The OOK modulation at the receiver coil is seen in Figure 4.3. Due to the relatively "clean" received waveform, the receiver device will be able to demodulate the OOK signal.

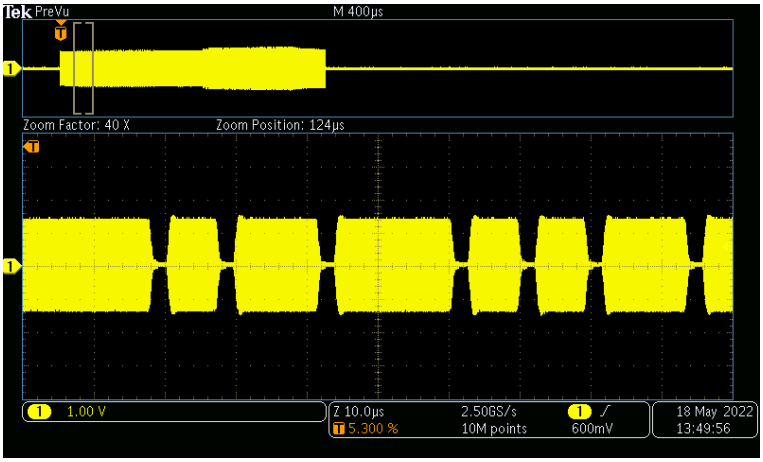

Figure 4.3: Voltage on the NFC receiver coil during the transmission of an OOK signal.

On the other hand, the receiver communicates information to the transmitter by modulating the load, i.e., the amount of power it taps from the generated magnetic field of the transmitter. This is called amplitude modulation (AM). This will directly affect the transmitter device as a change in reflected impedance. The term reflected impedance is in practice identical to what is described in Chapter 2, Section 2.2.3. The load modulation is seen in Figure 4.4.

To detect this change, the ST25R3916 chip has internal demodulation circuits. Both a peak detector and a quadrature demodulator are implemented. The load modulation is not as visible on the transmitter coil as the OOK is on the receiver coil. To identify the load modulation by probing the coils with the oscilloscope, the phase difference between the transmitter and receiver signal is probed. Outside load modulation, the phase difference between the two signals is 111 degrees, while inside the load modulation, that value is 127 degrees. This difference is what the demodulator uses to decode information sent by the receiving device.

A way of confirming that the correct information is communicated between the two NFC units is to activate logging in the firmware (FW), connect the NFC debugger to a PC, and listen on that specific communication port (COM). PuTTy is used for this purpose, and the communication log is seen below in Figure 4.5

[2]The decay time depends on a property of the resonant coil tank called the Q-factor. It is proportional to the inductance and inversely proportional to the resistance.

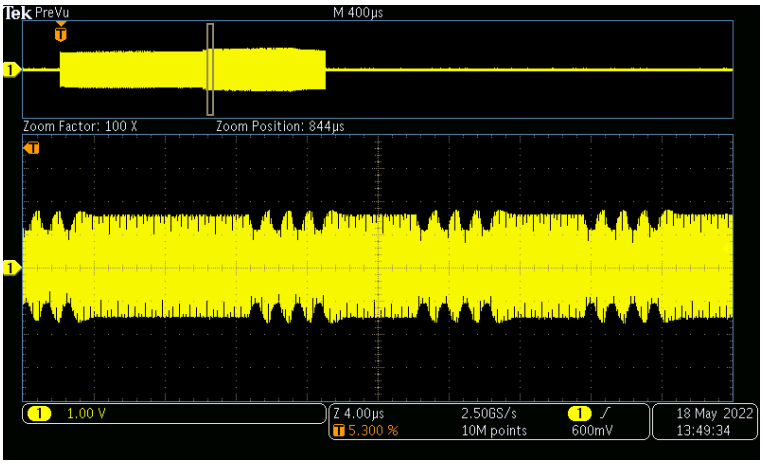

Figure 4.4: Voltage on the NFC receiver coil during receiver load modulation.

```
[1843164]Ki PTx State: KI_PTX_STATE_ACTIVATED (3)
[1843169]Ki PTx State: KI_PTX_STATE_START_CONFIGURATION (4)
[1843190] NDEF: D423107777772E776972656C65737370 6F776572636F6E736F727469756D2E636F6D3A776C6303100200000 1013AA6090A0B0
C0D0E1F
[1843201] WPC WLC Ki profile
        Version Number 0x10
        ALIVE FDT 2
        Read Data Buffer Start Address 0x00
        Write Data Buffer Start Address 0x00
        Read Data Buffer Size 1
        Write Data Buffer Size 1
        Read CMD Code 0x3a
        Write CMD Code 0xa6
        Maximum T_SLOT FOD 9
        Minimum T_POWER 10
        COMM_LAG_MAX 11
        Default T_SUSPEND 12
        Write Sequence Length 13
        Minimum Power 14
        Maximum Power 31
```

Figure 4.5: Example of communication of the Ki specific implementation of NFC.

4.4 Coil Production

4.4.1 NFC Coils

The NFC coils are manually winded as a pancake coil between two transparent polymer sheets. The wires used are defined in Chapter 3, Table 3.1. Previous work within the WPC was used as guidelines for determining the dimensions of the coils [3]. Both the transmitter and receiver coil are shown in Figure 4.6.

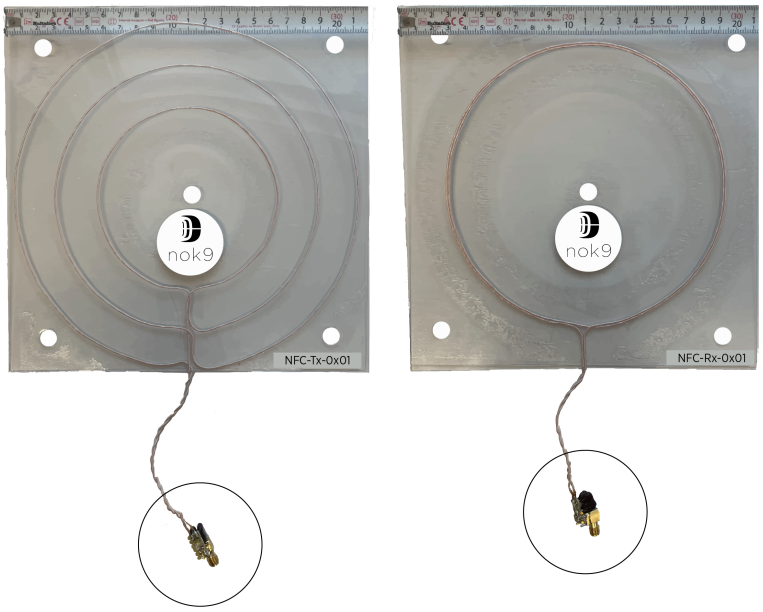

Figure 4.6: NFC-Tx-0x01 (left) and NFC-Rx-0x01 (right) together with the filter capacitor and SMA connector (circled).

There are five holes in the polymer sheets, which are for the fixture inside EVA III. The filter capacitors, along with the SMA connectors, are seen on both coils in the circled area. The SMA connector was used when characterizing the system with the VNA. During WPT and communication, the coils were directly soldered onto the NFC control system.

4.4.2 Main Coils

The main Tx coil (Ki-Tx-0x01) was manually wound on a 3D printed substrate, as seen in Figure 4.7. The main Rx coil is similar to the main Tx coil, but smaller. It is seen in Figure 4.8. The mechanical properties of both of these coils are found in Chapter 3, Table 3.1.

The coils are then mounted inside the EVA III MDT. The main Rx coil does not belong to the MDT unit, but in this case it will be mounted directly on the

[3] That work is not available to the public and will stay confidential within the WPC.

Figure 4.7: Ki-Tx-0x01.

Figure 4.8: Ki-Rx-0x01.

same fixture as the main Tx so to make the experimentation easier. The setup is depicted in Figure 4.9.

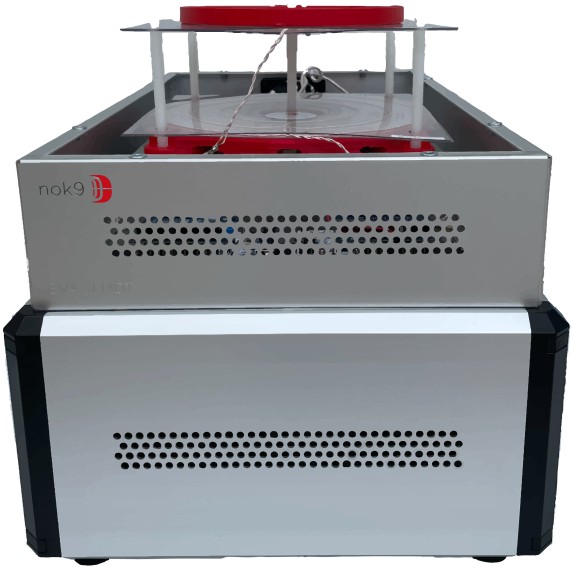

Figure 4.9: EVA III MDT with the main Tx, NFC Tx, NFC Rx, and main Rx coil mounted.

4.5 Decoupling

4.5.1 LC Filter

The decoupling filter is closely related to the characterization of the system described in Chapter 3 since the filters designed herein was included when characterizing the system. It was seen therein that the initial design did not perform as expected, and it was adjusted accordingly. In this section, the initial design and the adjustment are described.

Recall the theory on an LC filter in Section 2.5. Before building prototypes of the filtering circuitry, simulations of those circuits were performed in order to gain insight into the physical behavior of such circuits. The program LTSpice® is an open-source SPICE simulation tool developed by Analog Devices, which was used for this purpose[4].

The procedure for designing, building, and determining the electrical properties of a circuit prototype was as follows:

1. Determine desired circuit properties such as frequency response.

[4]This software does not include effects from EM fields. To incorporate simulations with EM effects, the simulations may be extended to include electromagnetic fields by utilizing other commercial programs such as COMSOL Multiphysics® or Altair FEKO.

2. Calculate component values to match the theoretical properties.
3. Simulate the circuit with those calculated values. Confirm that the simulation matches the calculation.
4. Construct the prototype and measure the properties. Most likely, the theory and reality will not be identical, and adjustments are to be expected[5].

Component Types

The type of components used to implement a filter for HF signals will impact on the robustness of the system behavior in terms of the frequency response, as certain types of components are not suitable for HF. Mica capacitors were used for the filter circuit. They are very stable for a wide range of frequencies and high temperatures, are well protected from moisture, and have low losses. However, for commercial implementation, class 1 ceramic capacitors (C0G) may be a good alternative; those are cheaper and more space-efficient.

Filter Design

The sole purpose of the filter is to suppress the LF signal induced from the main coils. And since those fields are expected to be very strong, this filter should be able to withstand such induced signals. The cut-off frequency f_c of the high-pass filter will be designed to be a bit below 13.56 MHz. Since the NFC coils will be the inductor in the LC-filter, those will set the value of the series capacitor after the desired f_c is set. When deciding on the capacitor to use, the inductance value of the coils, when mated, will be used. The filter in Figure 4.10 will yield a parallel resonance between the NFC-Tx-0x01 and Cs as calculated in Equation 4.1.

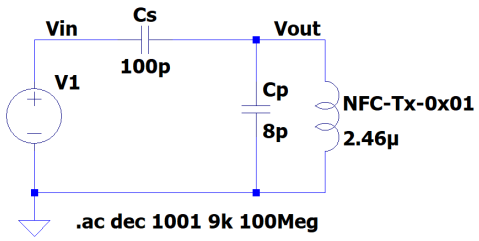

Figure 4.10: The equivalent circuit of the NFC-Tx-0x01, including the filter capacitor Cs.

$$f_0 = \frac{1}{2\pi\sqrt{2.46 \cdot 10^{-6} \cdot (100 + 8) \cdot 10^{-12}}} = 9.76 \text{ MHz}. \tag{4.1}$$

The transfer function of this filter can be calculated as a voltage division as below

[5]There would most likely be parasitic elements in the prototype that the simulation did not consider. Tolerances of components will also be added in the real components.

$$\frac{\text{Vout}}{\text{Vin}} = \frac{Z_{\text{NFC-Tx-0x01}}}{Z_{\text{NFC-Tx-0x01}} + Z_{\text{Cs}}} = \frac{\omega^2 LC}{\omega^2 LC - 1}, \tag{4.2}$$

where C, in this case, is 100 pF in parallel with 8 pF, which is 108 pF. To confirm that LTSpice and the equation yield the same results, both are plotted over frequency in Figure 4.11.

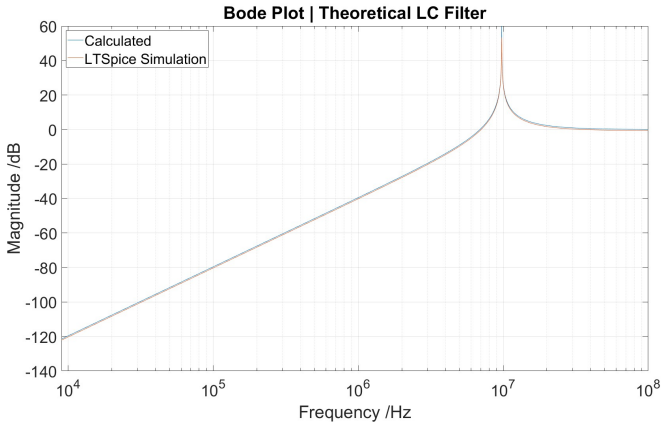

Figure 4.11: The magnitude of the output signal of a parallel LC filter with resonance at 9.76 MHz.

This resonance leaves a margin between the operating point and the resonance frequency; this capacitor value will be used in both NFC-Tx-0x01 and NFC-Rx-0x01[6]. In the same way, the resonance for NFC-Rx-0x01 is simulated and calculated.

Prototype Filter

The filter is built on an experiment board with the coil directly soldered onto it. The connection to the VNA is made through an SMA connector which also is soldered onto the experiment board. The initial design for both NFC-Tx-0x01 and NFC-Rx-0x01 was to use two 200 pF capacitors in series. As the mated measurements showed, the resonance of NFC-Tx-0x01 became too high, and one of the 200 pF capacitors was removed to decrease the resonance point. To point out the implications of the unexpected high resonance, no communications between the NFC-Tx-0x01 and NFC-Rx-0x01 with the initial filters were seen. When the filter was added only to NFC-Rx-0x01, the communication was successful, implying that NFC-Tx-0x01 has problems with the filter. When the adjusted filter was added to NFC-Tx-0x01, the communication was once again successful. The gap between NFC-Tx-0x01 and NFC-Rx-0x01 was at this point 39 mm, which is a realistic distance for future implementation.

[6]Note that the 100 pF may be achieved in reality by placing two 200 pF capacitor in series.

This adjusted filter has now demonstrated communication between the NFC devices using NFC-Tx-0x01 and NFC-Rx-0x01 as the coils and mounted in EVA III MDT with the main coils in place. Both main coils are in a short circuit state. If the main Rx coil is left open, the communication fails. The next step will be to activate the main coils to demonstrate successful NFC communication simultaneously as the main coils perform WPT at 45 kHz. Before activating the main coils, proper shielding of the NFC circuitry may be required to prevent damage to the NFC coils and/or circuitry.

4.5.2 Shielding Implementation

The theory of how to shield LF magnetic fields is well described in Chapter 2, Section 2.4. The tool used to investigate the extent of the fields and the effect of certain shielding implementations is called a spectrum analyzer (SA). This is a tool that is often used for EMC pre-compliance testing. By connecting a probe to the input of the SA, information about electromagnetic fields is directly presented, and a quick understanding of what kind of fields are present is the result. Both information about the frequency and if there are predominant electric or magnetic fields can be obtained. However, in this case, the magnetic fields are already known to be predominant magnetic, as the source is a low ohmic coil. The SA will be used to measure the difference in the spectrum with and without a shielding barrier. The absolute values are inconsequential since the probe was a custom-made coil of which the antenna factor is unknown[7].

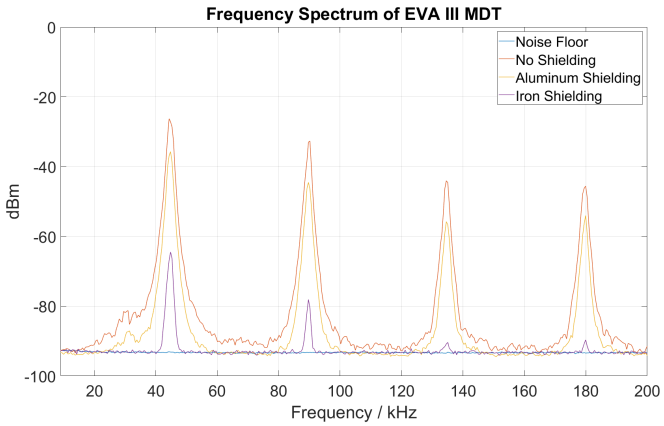

Figure 4.12: Shielding effectiveness of aluminum versus iron. Current probe is fixed during the measurements.

The probe was placed 20 cm from the main Tx coil in a fixed position, oriented orthogonal to the main Tx coil plane, and at the same horizontal height as the main Tx coil during the measurements. By comparing the magnitude of the signal at the

[7]The antenna factor is the ratio of field strength to the output voltage of the probe. This is a parameter that has to be calibrated for every probe, and over all frequencies the probes are to be operated at.

operating point when the 1 mm thick aluminum frame[8] is in place, versus when it is gone, it was seen that the signal strength was decreased, at the operating point, by 10 dBm or - 20 dBW. As expected, there is, in this case, a low shielding effect of a low permeable, conductive, and thin barrier. However, when a 2 mm thick steel cage (10x10x15 cm) was encapsulating the probe, the magnitude of the signal at the operating frequency was decreased by 40 dBm or ten dBW. A comparison is seen in Figure 4.12[9]. This iron cage will be used to encapsulate the NFC devices and the filtering circuitry. The spectrum is analyzed at a wider frequency span and is shown in Figure 4.13. At this point, the NFC devices and the filtering circuitry were all put inside the iron cage, the NFC Tx coil was mounted directly on top of the main Tx coil, and the NFC Rx coil was mounted with a gap of 10 mm from the NFC Tx coil.

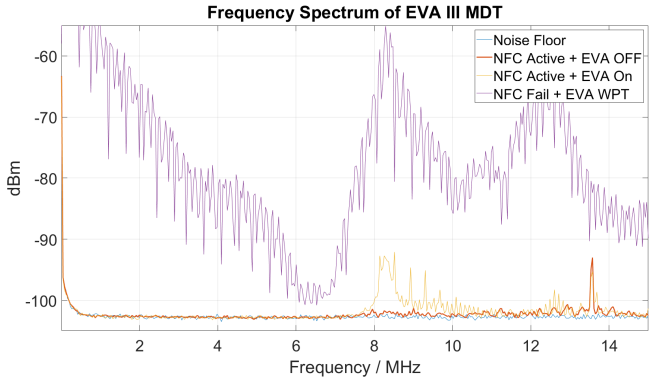

Figure 4.13: A comparison of the spectrum for various states of EVA III MDT and the NFC devices.

It can now be identified that the EM fields emitted from the main Tx coil will interfere significantly with the NFC coils and circuitry. For the red curve, the NFC transmitter and receiver are both active and they communicate without any errors. The peak signal is at 13.56 MHz[10]. When activating the EVA III MDT circuitry, and the main Tx coil is still not active; there appear to be EM fields from the electronics at 8 MHz and higher. This case is represented by the orange curve. At this point, the NFC communication is still functional. In the next state (purple in Figure 4.13), the 45 kHz WPT is activated, and instantly this effect is seen in the spectrum, even high up in the MHz range. NFC communication is now completely drowned in noise and there is no successful communication. In Figure 4.14, the SA is zoomed into the NFC area, and the probe was placed within the iron cage to see how much it shielded the HF content of the main Tx coil signal.

[8]That is the top part of EVA III MDT frame. This aluminum frame is removed completely and then mounted again during this comparison.

[9]In the figure, the spectrum was measured when EVA III MDT was operating in an open-loop at 45 kHz, without any receiver mated. The NFC coils were not active during these measurements.

[10]All measurements with the spectrum analyzer used the peak detector as detector

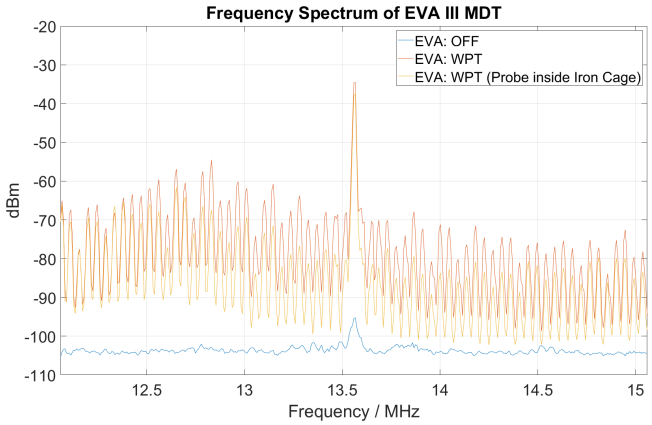

Figure 4.14: Effect of iron shielding at high frequency.

It is clear that the shielding effectiveness of the iron barrier is lower at 13 MHz as it is at 45 kHz (see Figure 4.12 for the shielding effect at kHz range).

4.6 Power Amplifier

4.6.1 Amplifier Topology

The specific topology of the amplifier will not be disclosed herein, as this is confidential information. The general principles may, however, be described. A push-pull amplifier will be used, built to be compatible with the NFC units described previously in Section 4.3. A push-pull amplifier is based on differential driving signals, meaning that the output stage can drive currents in both directions. This is typically implemented with metal-oxide-semiconductor transistors or similar. The advantage of a push-pull amplifier, in this case, is the low inserted distortion, meaning low interference with the modulated NFC signals.

4.7 Energy Harvester

In many receiving circuits of WPT, the harvesting is done through a simple diode rectifier. This usually implies a voltage drop of around 0.5-0.7 volt. For low currents, the losses in a diode rectifier may not be significant. A typical diode rectifier is illustrated in Figure 4.15

However, to minimize the losses, a synchronous rectifier may be implemented. This means replacing the passive diodes with active devices: transistors. The voltage drop over a saturated transistor can be arbitrarily low, and the losses can be omitted. The price of such a rectifier is higher; the design is more complex as additional circuitry is required. Without the additional circuitry, the synchronous

setting, meaning low duty cycle pulses will still appear in the spectrum.

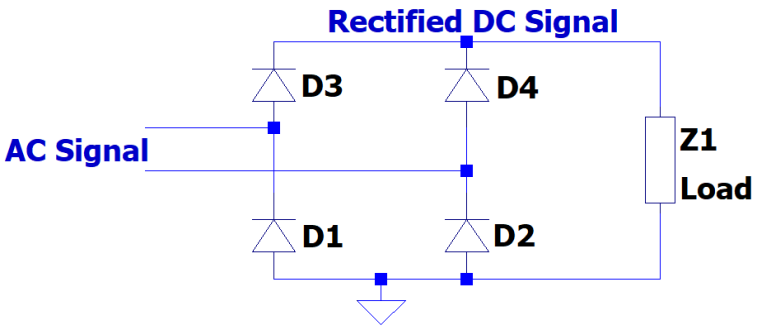

Figure 4.15: A simple diode rectifier.

rectifier will look identical to the diode rectifier, with the exception of transistors being used instead of diodes.

The load Z1 in Figure 4.15 may be an electronic load that can operate in various modes, such as constant voltage or constant current. A buffer capacitor may also be added to the rectified signal to achieve a stable DC voltage level.

Chapter 5
Benchmark & Discussion

The first thesis goal of true coexistence has not been demonstrated herein. This goal was the first of two and had the highest priority, meaning that neither of the goals had been achieved. However, the work presented herein may be used as a guide for future work to achieve these two goals. A breakthrough in the technology underlying cordless kitchen appliances will require coexistence-related issues to be solved.

5.1 Benchmark

The setups that yield successful communication[1] are defined so that benchmarking may be performed to compare different implementations and techniques. The performance to benchmark will be the distance between the transmitter coil and receiver coil, which results in successful communication. The coils will, in this case, always be co-centered (the coil axes should align with one another). The coils will also be mounted in the EVA III MDT device at all times during the performance measurements. EVA III MDT will be turned on at all times during the performance measurements, but the main Tx coil will not be active. The LC filters described will be connected at all times. The coils will be positioned as illustrated in Figure 4.9. The communication should be successful for these three cases:

- Ki-Tx-0x01 is connected by default to inverter output. NFC-Tx-0x01 is placed on top of Ki-Tx-0x01. NFC-Rx-0x01 is placed with 80 mm distance to NFC-Tx-0x01. Ki-Rx-0x01 is not present.

- Ki-Tx-0x01 is connected as default to inverter output. NFC-Tx-0x01 is placed on top of Ki-Tx-0x01. NFC-Rx-0x01 is placed with 58 mm distance to NFC-Tx-0x01. Ki-Rx-0x01 is placed on top of NFC-Rx-0x01 (open circuit).

[1] Successful communication is achieved if the Tx can decode the specific NDEF information of the Rx, and continuously poll the Rx for data.

- Ki-Tx-0x01 is connected as default to inverter output. NFC-Tx-0x01 is placed on top of Ki-Tx-0x01. NFC-Rx-0x01 is placed with 58 mm distance to NFC-Tx-0x01. Ki-Rx-0x01 is placed on top of NFC-Rx-0x01 (short circuit).

The typical distance expected between the transmitter and receiver coils depends on whether a hob or hidden case is used. In the hidden case, a thick kitchen counter will add extra distance. For reference, a typical distance in the hob case is 20-30 mm.

5.2 Importance of In-Circuit Measurements

It has become apparent from the results of Chapter 3 that there is a significant difference in the electrical properties of the coils when they are located in air compared to when located inside EVA III MDT. The inductive coupling to nearby coils and other materials will effectively change the circuit parameters of the coil. The LC filter was first designed assuming the coils are surrounded by only air, and it was observed that the filter did not behave as expected when the NFC coils were placed inside EVA III MDT. Had the filter been designed with the inductance value as measured when located inside EVA III MDT, it would have worked directly without modification.

5.3 Further Characterization

The system had been characterized as passive components without any of the coils being active. When using the VNA to measure the properties of the NFC coils, the main coils are either open or short-circuited. This will not be the case during WPT. A relevant comparison would be to investigate how the impedance of the NFC coils changes when the main coils are active and operational. This would, however, require caution as the VNA ports are rated for maximum 27 dBm input power. At a 50 Ohm termination, that is 5 V RMS. The main coils may induce far higher voltage levels than 5 V, and so an attenuator will be required along with careful testing. The assumption when doing the characterization was that the corner cases would be when the main coils are open and shorted, but this may not be the case.

Chapter 6
Conclusions and Future Work

6.1 Overall Conclusions

A system for WPT that can, through the main transmitter and receiver coil, transmit power levels of up to 2.5 kW along with a system for communication has been built to investigate the coexistence between the two said systems. Since the two systems operate at different frequencies, it was expected that they would be able to operate simultaneously if proper filtering and shielding were implemented. The first goal of this thesis was to demonstrate the coexistence between the two systems. This would be demonstrated using a prototype able to transmit up to 2.5 kW of power through WPT while simultaneously communicating through the NFC standard using a second system that is closely integrated with the high-power system. The second goal was to enable low-power energy harvesting through the communication link. The first goal had the highest priority, and to achieve this goal, a filter in the form of a high-pass LC filter was implemented for the communication system to prevent conducted interference. For radiated interference, a high-permeable material was used to shield against LF magnetic fields. Despite these two implementations, the two systems could not successfully operate simultaneously. The communication fails instantly when the high-power WPT is activated. The reason for this is unknown, but there are at least three possible explanations. One explanation is that the filtering is not sufficient, meaning that the noise from the high-power WPT will drown the communication signal and thus preventing successful communication. Another explanation is that the shielding is not attenuating the EM fields sufficiently and thus these fields create noise in the communication circuitry. The last explanation is that the electrical properties of the communication coils may change significantly when the high-power WPT is activated as compared to when the coils of the high-power WPT are either short-circuited or open-circuited. This change may be enough to make the coils capacitive, as the filtering has been designed with relatively narrow margins. There may be another explanation for the communication failure. However, as it have been seen that the electrical properties of the NFC coils are quite sensitive to what is surrounding the coils, the third explanation may be interesting to investigate further by characterizing the communication system when the main WPT system is active, as discussed in Section 5.3.

A proper design is needed to achieve true coexistence between the main high-

power coils and the NFC communication coils. If the convenience of having the two systems operate simultaneously outweighs the solution where the two systems are separated in time is yet to be proven. Separating the systems in time will be effective and will not require such robust shielding between the two systems. However, it will not be ideal as this implies a lower data transfer rate and also a lower power transfer through the NFC link. The two systems were not able to operate simultaneously, and so true coexistence was not achieved. Neither was the second goal of low-power energy harvesting achieved. However, a path for future work on achieving the first goal is provided below.

6.2 Improvements for Future Work

With the results presented within Chapter 3 and Chapter 4, the improvements needed to achieve the true coexistence goal are better understood.

6.2.1 Shielding

The shielding was designed to suppress LF magnetic fields, as that is what the main coils will emit due to the change in current. However, to create this LF current change, the inverter will switch the voltage of the coil at an HF. This is seen in Figure 6.1.

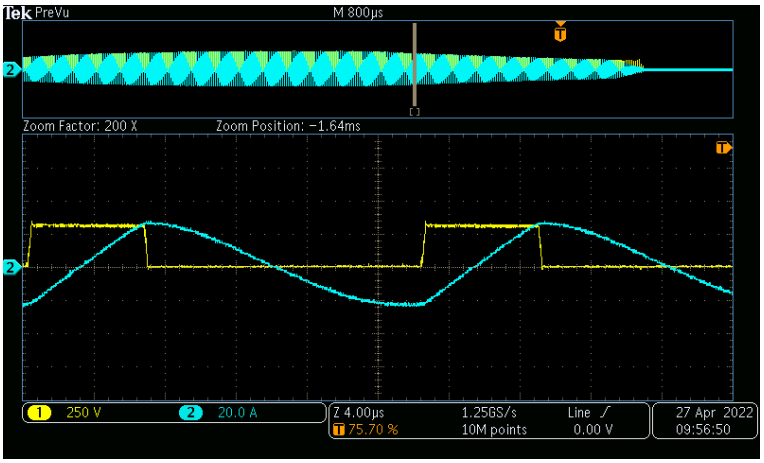

Figure 6.1: Ki-Tx-0x01 current (turquoise) and voltage (yellow).

The yellow trace is the voltage of the switching node of a half-bridge inverter configuration. The HF voltage switching will, together with the LF current signal, create EMI for the NFC coils and circuit. The shielding was designed to suppress mainly the LF magnetic fields, but the HF electric fields must also be suppressed. The frequency content of the current and voltage is compared in Figure 6.2.

This figure confirms that the HF fields seen back in Section 4.5.2 were electric fields generated by the inverter switching voltage. Thus, the barrier used to shield

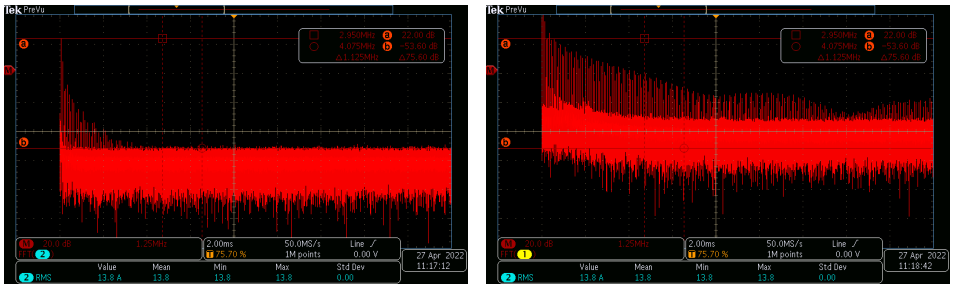

(a) (b)

Figure 6.2: Frequency content of the current (a) and voltage (b) in the main Tx coil during WPT.

these fields should be a low ohmic material such as aluminum. Therefore, the shield should be designed for both LF magnetic fields and HF electric fields.

6.2.2 LC Filter

The filter is simply a series capacitor that, together with the coil, forms a second-order high pass filter. To thoroughly test whether the filter, the shielding, or both is the Achilles' heel, the NFC circuitry may be placed at a long distance from the main coils. The coils will need an extension cable which will induce inductance, and so the filter should be adjusted with this in mind. If the communication stops working when the main coils enter WPT, it is due to the conducted interference rather than the emitted interference. If it works, then the radiated interference is the cause, and the focus should be on improving the shielding.

6.2.3 Coil Impedance Tuning

The NFC driving circuitry consists, among other parts, of an impedance matching network. This matching aims to adjust the load impedance to the source impedance to minimize any reflections that would decrease the amount of power delivered to the load, which is, in this case, the coil. This relates to what was discussed in the theory of waves and their impedance.

In this setup, the matching network is designed by ST for their default printed coil. However, the NFC coils used in this work are not identical to the original ones in NFC-Tx-0x01 nor NFC-Rx-0x01, so there will be a mismatch between the source and load impedance which will cause reflections. There are ways of calculating the appropriate matching network components[1]. Note that the series capacitor used in the filter should be included in the load impedance when calculating the matching impedances.

[1] An application note from Würth Elektronik explains the procedure for impedance matching network. See the application note named "ANP084" by Christian Merz.

6.2.4 Power Amplifier

To minimize the risk of the NFC signal drowning in the noise from the main LF signal, the field strength of the NFC signal may be increased. This is what the power amplifier can do. As a positive side-effect of the requirement of 500 mW power transferred through the NFC link, the signal of the communication carrier will be strengthened.

References

[1] J. Clerk Maxwell, "A dynamical theory of the electromagnetic field," *Phil. Trans. R. Soc. Lond.*, Vol. 155, 459-512, ISSN: 2053-9223, 1865.

[2] D. L. Sengupta, T. K. Sarkar, "Maxwell, Hertz, the Maxwellians, and the early history of electromagnetic waves," *IEEE Antennas and Propagation Magazine*, Vol. 45, Nr. 2, 13-19, 2003.

[3] B. J. Hunt, *"The Maxwellians,"* Cornell University Press, 2005.

[4] A. S. Marincic,"Nikola Tesla and the wireless transmission of energy," *IEEE Transactions on Power Apparatus and Systems,* Vol. 10, 4064-4068, 1982.

[5] NFC Forum, *"NFC Forum adds certification for NFC wireless charging",* 2020, `https://www.nfcw.com/nfc-world/nfc-forum-adds-certification-for-nfc-wireless-charging/`

[6] A. Wageningen, A. Staring, 2016, Inductive wireless power transfer with time slotted communication, US Patent 10,396,595 B2.

[7] D. Askeland, W. Wright, *"The Science and engineering of materials, Seventh edition",* Cengage Learning, Global Engineering, ISBN: 978-1-305-07676-1, 2014.

[8] J. Acero, C. Carretero, I. Lope, R. Alonso, Ó. Lucia and J. M. Burdio, "Analysis of the Mutual Inductance of Planar-Lumped Inductive Power Transfer Systems," *IEEE Transactions on Industrial Electronics*, Vol. 60, Nr. 1, pp. 410-420, 2013.

[9] J. Zwinkels, "Light, electromagnetic spectrum." Encyclopedia of Color Science and Technology, pp. 843-849, 2015.

[10] R. Lambourne, "Elecricity, Relativity and Magnetism: a unified text," *Physics Education*, Vol. 34, Nr. 5, 1999.

[11] H. Hayt, *"Engineering Electromagnetics",* McGraw-Hill, 1989.

[12] G Igal, D. Kaplan, and Y. Lehavi. "Teaching Faraday's law of electromagnetic induction in an introductory physics course." *American journal of physics*, pp. 337-343, 2006.

[13] E. Kriezis, T. Tsiboukis, S. Panas, J. Tegopoulos, "Eddy Currents: Theory and Applications," *Proceedings of the IEEE*, Vol. 80, Nr. 10, 1559-1589, 1992.

[14] L. C. Meng, E. Cheng, and K. W. Chan. "Heating performance improvement and field study of the induction cooker." *2009 3rd International Conference on Power Electronics Systems and Applications*, PESA, 2009.

[15] T. Campi, S. Cruciani, F. Maradei and M. Feliziani, "Wireless Charging System Integrated in a Small Unmanned Aerial Vehicle (UAV) with High Tolerance to Planar Coil Misalignment," *2019 Joint International Symposium on Electromagnetic Compatibility, Sapporo and Asia-Pacific International Symposium on Electromagnetic Compatibility*, pp. 601-604, 2019.

[16] B. Hesterman, "Mutual Resistance", *Utah State University*, 2020, `https://verimod.com/presentations/Mutual_Resistance_Rev3.pdf`

[17] Wireless Power Consortium, *Qi Specification: Communications Protocol, Version 1.3*, `https://www.wirelesspowerconsortium.com/knowledge-base/specifications/`

[18] Keysight, *The Evolution of RF/Microwave Network Analyzers*, `https://about.keysight.com/en/newsroom/backgrounders/na/`

[19] T. Willims, *"EMC for Product Designers",* Elsevier Ltd, ISBN 978-0081010167, 2017.

[20] J. Castro-Ramos, et al, "The refraction and reflection laws from a complete integral of the eikonal equation and Huygens' principle," Journal of Optics, Vol 17.1, 015601, 2014.

[21] D. M. Pozar, *"Microwave Engineering"*, 3rd edition, J. Wiley, 2005.

[22] X Nan, C. R. Sullivan, "An improved calculation of proximity-effect loss in high-frequency windings of round conductors," *IEEE 34th Annual Conference on Power Electronics Specialist*, Vol. 2, 853-860, 2003.

[23] NFC Forum, *"History of Near Field Communication"*, 2004, `http://nearfieldcommunication.org/history-nfc.html`

Appendix A

Decoupling Filter

Resonance in an LC circuit is defined as the angular frequency $\omega_0 = 2\pi f_0$ at which the reactance of the inductor equals the reactance of the capacitor:

$$X_L = -X_C \Leftrightarrow j\omega_0 L = \frac{1}{j\omega_0 C} \Leftrightarrow \omega_0 = \frac{1}{\sqrt{\mathrm{LC}}} \tag{A.1}$$

In Figure A.1 a), the impedance is

$$Z_{\mathrm{par}} = \frac{X_C X_L}{X_C + X_L} \Rightarrow \lim_{\omega \to \omega_0} Z_{\mathrm{par}} = \infty \tag{A.2}$$

In Figure A.1 b), the impedance is

$$Z_{\mathrm{ser}} = X_L + X_C \Rightarrow \lim_{\omega \to \omega_0} Z_{\mathrm{ser}} = 0 \tag{A.3}$$

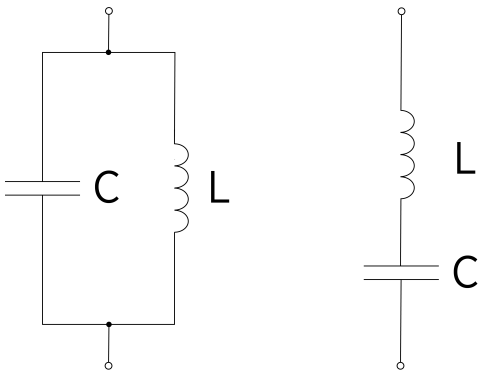

Figure A.1: Two LC Filters. a) Parallel LC circuit. b) Series LC circuit.

Printed by Tryckeriet i E-huset, Lund 2022

LUND
UNIVERSITY

Series of Master's theses
Department of Electrical and Information Technology
LU/LTH-EIT 2022-890
http://www.eit.lth.se